23rd ABCM International Congress of Mechanical Engineering
December 6-11, 2015, Rio de Janeiro, RJ, Brazil

# INTEGRATED OPTIMIZATION STUDY OF AXIAL EXPANDER APPLIED TO WASTE HEAT RECOVERY SYSTEM

**Guilherme Leibsohn Martins**
Petrobras – Av. Henrique Valadares, 28 – Centro – Rio de Janeiro/RJ - Brasil
guileibsohn@petrobras.com.br

**Sergio Leal Braga**
Pontifícia Universidade Católica do Rio de Janeiro – Av. Marquês de São Vicente, 225 – Gávea – Rio de Janeiro /RJ – Brasil
slbraga@puc-rio.br

**Sandro Barros Ferreira**
GT2 Energia – Av. Das Américas 500, bloco 15/201 – Barra da Tijuca - Rio de Janeiro / RJ – Brasil
sandro@gt2.com.br

***Abstract.*** *An analysis of the application of an organic Rankine cycle (ORC) to recover the heat rejected by an internal combustion engine is presented. The selected fluid is R245fa, whose real gas behavior is relevant under the studied conditions, as modeled by the Redlich-Kwong-Soave equation of state. A single stage partial admission axial expander is assumed to directly drive a synchronous two pole generator. The loss model for the flow through the axial blades adopted in this work is based on the boundary layer theory, the concept of diffusion factor, wind tunnel cascade tests available in literature and the conservation equations for compressible flow. The basic geometry and dimensions needed to achieve maximum expander efficiency are determined under several subcritical and supercritical cycle conditions by means of a restrained design optimization algorithm. The optimum value for the evaporator temperature is stablished so as to obtain the maximum power from the subcritical cycle, according the constructive alternatives considered. The single stage expander design is shown to be greatly influenced by media compressibility and the use of convergent-divergent profiled nozzles is promising to achieve the highest possible performance potential, especially at high pressure steam generator conditions.*

***Keywords:*** *organic Rankine cycle, waste heat recovery, dense gases, design optimization, axial stage efficiency.*

## 1. INTRODUCTION

Waste heat recovery from an internal combustion engine may be achieved by an organic Rankine cycle (ORC) system, as illustrated in Fig. 1. Unlike the conventional Rankine cycle, an organic fluid is used as working fluid, which may be a paraffinic or aromatic hydrocarbon, a refrigerant fluid, ammonia-water mixture or a new generation of silicon based fluids. In general the organic fluids present a positive slope in the saturated steam curve at the temperature-entropy diagram, which will make the expander exhaust to be overheated. A single stage backpressure expander is required for these conditions, in opposition to the multiple stages condensing expander used in the conventional Rankine cycle. Furthermore, a minimum amount of overheat is needed at expander inlet, which makes the ORC more competitive for heat recovery at low and medium temperature.

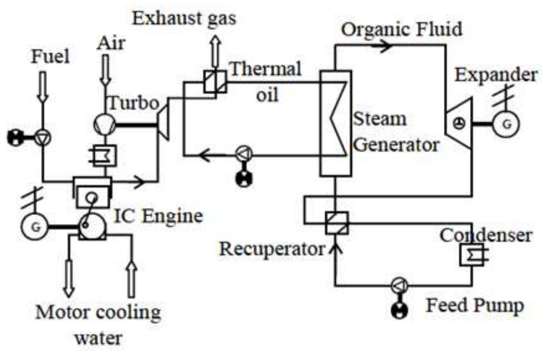


Figure 1. Waste heat recovery scheme applied to an internal combustion engine (Schuster et al., 2009).

In heat recovery application an intermediary thermal fluid must be used to avoid contact of the organic fluid with the high temperature engine exhaust. This heat exchange system is usually designed considering a pinch point between the thermal oil and the organic fluid, which is physically located at evaporator inlet. Another pinch point relating the exhaust gas and the thermal oil is also considered and it is supposed to be located at the exit of the stack heat exchanger.

The traditional approach of cycle analysis considers a constant efficiency level for the expander (Chao, et al., 2012). In fact this behavior may be at least partially achieved by increasing the number of stages, as required by the increase of steam generator pressure. The consequence is an increase of the equipment complexity and cost. In this work it is assumed a single stage axial expander, such way its efficiency is expected to be closely related to the cycle operating conditions. The single stage expander will be preliminarily designed to achieve the maximum possible efficiency under each specified cycle conditions. This way an integrated optimization performance procedure is intended to be simultaneously applied to cycle and expander.

## 2. APPLICATION STUDY

The case studied consists of an ORC heat recovery system using R245fa as working fluid, to be applied in a commercial internal combustion engine of the 2 MW class. The exhaust gas is available at temperature of 511ºC and standard volumetric flow of 9420 Nm3/h. A partial admission axial expander is considered to directly drive a synchronous two pole electrical generator, under the motivation of lower cost equipment and the manufacturing capability of the local industry.

Some premises are adopted for the cycle as described below:

- For the evaporator temperature from 80ºC to 120ºC, an overheating of 5ºC at expander inlet will be enough. For higher evaporator temperatures, 10ºC of overheating is considered;
- The organic fluid is condensed at 50ºC;
- The temperature difference at pinch points are considered as follows: 40ºC between flue gas and thermal oil and 10ºC between organic fluid and thermal oil;
- Pump efficiency is supposed to be 75%.

A pinch point is characterized by the same slope in the temperature versus heat transferred curves for both fluids involved. Under these assumptions the temperature evolution at the hot source heat exchangers are outlined in Tab. 1, according to the specified evaporator temperature. Inlet and outlet temperatures and mass flow for the exhaust gas, the thermal oil and the organic fluid, the rate of heat transferred *Q* and the isentropic enthalpy drop available for the expander $\Delta h_{is}$ are shown. The temperature evolution versus the fraction of heat transferred for the three fluids at an evaporator temperature of 140ºC is illustrated in Fig. 2.

Table 1. Operation of the heat exchange system at subcritical cycle.

| Exhaust gas | | | | Thermal oil | | | Organic fluid | | | | |
|---|---|---|---|---|---|---|---|---|---|---|---|
| $T_{in}$ (ºC) | $T_{out}$ (ºC) | $\dot{m}$ (kg/s) | Q (kW) | $T_{in}$ (ºC) | $T_{out}$ (ºC) | $\dot{m}$ (kg/s) | $T_{evap}$ (ºC) | $T_{in}$ (ºC) | $T_{out}$ (ºC) | $\dot{m}$ (kg/s) | $\Delta h_{is}$ (kJ/kg) |
| 511,0 | 100,7 | 3,496 | 1612,4 | 60,7 | 188,2 | 6,406 | 80,0 | 50,3 | 85,0 | 7,989 | 15,59 |
| 511,0 | 101,4 | 3,496 | 1609,8 | 61,4 | 191,0 | 6,278 | 90,0 | 50,4 | 95,0 | 7,719 | 20,26 |
| 511,0 | 102,5 | 3,496 | 1605,4 | 62,5 | 193,0 | 6,203 | 100,0 | 50,5 | 105,0 | 7,469 | 24,69 |
| 511,0 | 104,6 | 3,496 | 1597,7 | 64,6 | 194,2 | 6,200 | 110,0 | 50,8 | 115,0 | 7,236 | 28,81 |
| 511,0 | 108,1 | 3,496 | 1584,6 | 68,1 | 194,2 | 6,305 | 120,0 | 51,0 | 125,0 | 7,010 | 32,62 |
| 511,0 | 114,5 | 3,496 | 1560,5 | 74,5 | 192,3 | 6,624 | 130,0 | 51,2 | 135,0 | 6,775 | 36,15 |
| 511,0 | 119,8 | 3,496 | 1540,6 | 79,8 | 190,2 | 6,956 | 135,0 | 51,4 | 140,0 | 6,641 | 37,70 |
| 511,0 | 127,6 | 3,496 | 1510,9 | 87,6 | 190,6 | 7,274 | 140,0 | 51,5 | 150,0 | 6,243 | 40,70 |
| 511,0 | 140,3 | 3,496 | 1463,2 | 100,3 | 185,5 | 8,460 | 145,0 | 51,7 | 155,0 | 6,008 | 42,22 |
| 511,0 | 162,7 | 3,496 | 1378,0 | 122,7 | 177,2 | 12,355 | 150,0 | 51,9 | 160,0 | 5,632 | 43,64 |

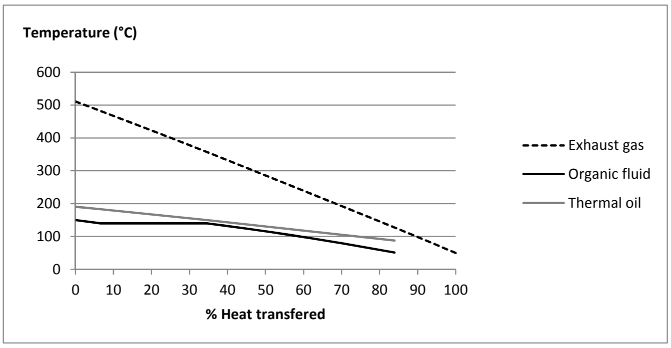


Figure 2. Engine exhaust gas, organic fluid and thermal oil temperature evolution versus the fraction of heat transferred at 140ºC ORC evaporator temperature.

## 3. REAL GAS EFFECTS

The real gas behavior of R245fa is relevant under the studied conditions, especially near the critical point where the dense gas condition is reached. The use of the Redlich-Kwong-Soave equation of state is indicated by Luján, et al. (2012) to satisfactorily represent the non-ideal effects of R245fa fluid. This fact is confirmed by observing in Fig. 3 that RKS results for the enthalpy and entropy departure functions are virtually the same as those from NIST database. The non-dimensional departure functions are plotted versus the reduced pressure for the isothermal at reduced temperature equal to 1,014. The results obtained from the Lee-Kesler equation of state are also shown for comparison.

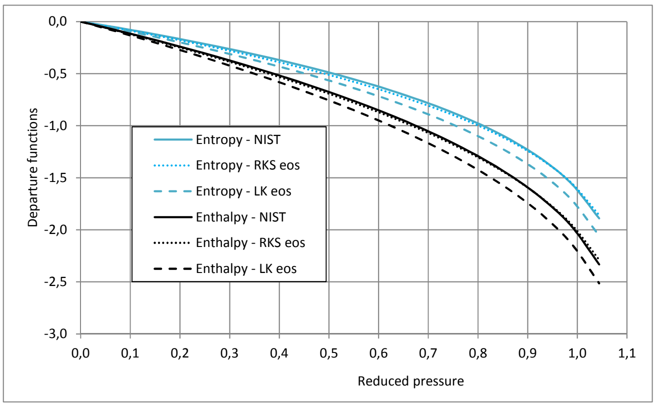


Figure 3. Enthalpy and entropy departure functions at reduced temperature equal to 1,014 from RKS and Lee-Kesler (Lee and Kesler, 1975) equations of state compared to values from NIST database for the R245fa fluid.

The correspondent aero-thermal equations are derived relating the temperature and pressure stagnation to static ratio $T_0/T$ and $p_0/p$ to the flow Mach number $M$. The non-ideal effects are accounted through the contribution of the enthalpy and entropy departure functions $\Delta h_{dep}/RT_c$ and $\Delta s_{dep}/R$ and the compressibility factor Z, being $R$ the gas constant and $T_c$ the critical temperature.

$$\frac{T_0}{T} = \frac{1+\left(\frac{k^*-1}{k^*}\right)\frac{k}{2}ZM^2}{1+\frac{k^*-1}{k^*}\left(\frac{\Delta h_{dep,0}/RT_c - \Delta h_{dep}/RT_c}{T_0/T_c}\right)} \tag{1}$$

$$\frac{p_0}{p} = e^{\left(\frac{\Delta s_{dep,0}}{R}-\frac{\Delta s_{dep}}{R}\right)}\left(\frac{T_0}{T}\right)^{\frac{k^*}{k^*-1}} \tag{2}$$

The presented expressions are obtained from a constant value of the ideal gas state isentropic exponent $k^*$. They are also acceptable when this parameter show a linear dependency on temperature, if it is evaluated at an equivalent value given by the arithmetic mean for Eq. (1) or by the logarithmic mean for Eq. (2). A variation of less than 3% in $k^*$ is verified for the R245fa under the cycle conditions studied in this work, validating the above premise. The real gas state isentropic exponent $k$, otherwise, is highly influenced by temperature and pressure, assuming a lower value as the fluid approaches the critical point. The large variation in $k$ affects the sound speed as described by the fundamental derivative of gas dynamics (Colonna et al., 2009). Unlike the ideal behavior, a dense gas will experience an increase in the sound velocity along an isentropic expansion (Wheeler and Ong, 2013).

## 4. AXIAL EXPANDER PERFORMANCE

The ORC axial expander performance estimation is based on the determination of the velocity diagrams. The performance estimation is intended to be done as a preliminary meanline design (Zhdanov et al., 2013) and it shall be dependent only on few geometrical parameters, like the meanline curvature length to chord ratio $l/C$ and the cascade solidity $\sigma$, defined as the chord length to blade spacing ratio. The velocity vectors are calculated at stations located upstream and downstream of each blade row, where the flow is supposed to be circumferentially uniform. For a known upstream velocity $V_{up}$, the downstream velocity $V_{down}$ is determined taking into consideration the amount of thermal energy converted into kinetic energy, the mass conservation and the kinetic energy loss coefficient for that specific blade row. The axial stage velocity diagram is characterized by some parameters as the axial acceleration factor and the degree of reaction. The axial acceleration factor is defined as the ratio of downstream to upstream rotor axial velocities and the degree of reaction is defined by the ratio of the energy converted in the rotor channel to the total energy available for the stage. The axial acceleration factor depends on the specific mass ratio and the meridional area ratio through the rotor blade.

The flow loss model adopted in this work is based on the growth of boundary layer momentum thickness due the occurrence of diffusion on the blade profile surfaces. A non-dimensional momentum thickness is obtained by dividing it by the mean camberline length *l*. A correlation between the $\vartheta/l$ and a diffusion parameter specifically stablished for axial turbine blades was presented by Stewart, et al. (1960), based on low speed cascade tests (Dunavant and Erwin, 1956) and also on design data of transonic rotor blades (Stewart, et al., 1960), as given by Eq. (3). The diffusion parameter $D_{tot}$ proposed was called total diffusion factor, taking into account the amount of diffusion in both pressure (concave) and suction (convex) blade surfaces.

$$\frac{\vartheta}{l} = \frac{0{,}003}{1 - 1{,}4 D_{tot}} \tag{3}$$

The flow through a blade cascade is realized to be a superposition of a uniform field and a circulatory field, such way a correlation can be stablished between the maximum surface profile velocity to upstream velocity ratio and a circulation parameter. This parameter is suggested by the application of the Kelvin circulation theorem in the inter-blade channel. It follows that the circulation around one blade can be represented by the product of the blade spacing by the difference of downstream to upstream tangential velocities $\Delta V_u$. A non-dimensional parameter is obtained if the circulation is divided by the product of the upstream velocity and the blade chord. A linearized correlation intended to be generically applied for all axial cascades was proposed (Baljé, 1968), which was based on a circulation parameter projected in the axial direction and on decelerating cascade experimental data. When applying this method to accelerating cascades, however, the loss estimation seems to be conservative. The slope coefficient as well the circulation parameter originally proposed were revised (Martins, et al., 2015) by analyzing the turbine blade cascade tests presented by Dunavant and Erwin (1956). The resulting expression for the equivalent diffusion factor is given by the following expression, where $d_{max}/C$ is the cascade thickness to chord ratio:

$$D_{tot} = 1 - \frac{V_{down}/V_{up}}{1 + 0{,}9\dfrac{d_{\max}}{C} + 1{,}4\dfrac{\Delta V_u}{\sigma V_{up}\, l/C}} \tag{4}$$

After calculating the equivalent diffusion factor from Eq. (4), the entire set of experiments were satisfactorily matched to Stewart correlation given by Eq. (3), as shown in Fig. 4.

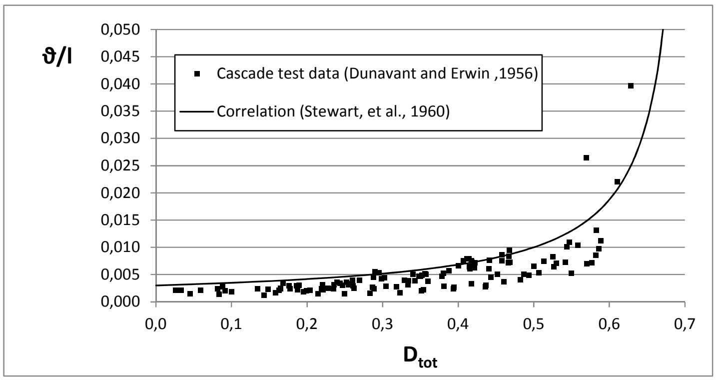


Figure 4 – Matching of experimental data (Dunavant and Erwin, 1956) to the non-dimensional momentum thickness versus diffusion factor correlation (Stewart, et al., 1960).

From the profile momentum thickness determined as the above description, a tridimensional momentum thickness parameter can be obtained taking into consideration further the boundary layers developed along the end walls. From mass and momentum conservation equations before and after mixing boundary layers with free stream, a total pressure ratio is obtained and then the kinetic energy loss coefficient is stablished. The overexpansion loss resulting from supersonic exit flow in convergent blades has also to be considered. Disk friction and partial admission losses are further taken into account. The proposed loss model was validated through the comparison with some traditional methods published, with experimental results in cascades and turbine stages and with results from factory bench tests of commercial single stage steam turbines.

## 5. EXPANDER OPTIMIZATION CRITERIA

The optimum expander design comprises the determination of the stage geometry required to obtain the maximum possible efficiency under the known operating conditions. Stage efficiency calculation is based on the velocity diagrams and loss estimation methods described in the preceding section. The optimum efficiency potential of an axial turbine stage is usually expressed as function of the non-dimensional similarity parameters specific speed $N_s$ and specific diameter $D_s$, defined by Eq. (5) and Eq. (6), respectively. The specific speed is the parameter responsible to specify the service conditions for which the stage is intended to work, to know: the rotational speed $\Omega$, the enthalpy drop available $\Delta h_{is}$ and the volumetric flow at rotor blade exit $Q_3$. The specific diameter incorporates the effect of the selected blade tip diameter $D$ and it shall be optimized for those conditions represented by the specific speed, unless some added restriction enforces it to assume a non-optimum value.

$$N_s = \frac{\Omega Q_3^{1/2}}{\Delta h_{is}^{3/4}} \quad (5)$$

$$D_s = \frac{D \Delta h_{is}^{1/4}}{Q_3^{1/2}} \quad (6)$$

The efficiency potential of partial admission axial stage under incompressible media and minimum loss criteria is stablished by Baljé and Binsley (1968). Macchi and Perdichizzi (1981) have studied the full admission axial stage optimization under nonconventional fluids considered as a perfect gas, once geometry and performance cannot be anticipated based on previous experience. The present work adds the real gas and compressible media effects to the partial admission stage design. The variable to be maximized is the total to static efficiency, once the exit kinetic energy is not supposed to be recovered. A flared blade design or a lap arrangement is predicted to accommodate the large volume ratio at which the stage is expected to be subjected under the ORC operation. The lap ratio is defined as the rotor height to nozzle height ratio.

Two restrictions associated with media compressibility are imposed to ensure acceptable performance: a limit aerodynamic load for a convergent blade and a limit inlet flow condition for a transonic blade. A convergent profiled blade cascade is able to produce supersonic flow at exit by means of a Prandtl-Mayer corner expansion around the trailing edge. A maximum exit Mach of 1,4 is stablished for stationary as well for rotating convergent profiled blade. A supersonic inlet flow shall be avoided for a transonic blade, as it must be free of shock waves while turns across the blade channel. A maximum inlet Mach number of 0,8 is stated for rotating blades, although this value may be considered somewhat conservative for a low specific speed stage.

Geometrical restrictions are also considered to ensure an efficient flow path as well a feasible manufacture, like a maximum flare angle of 7º and a minimum throat width of 3 mm. Some other variables are set to constant values, as a nozzle exit flow angle of 15º and a trailing edge thickness equal to 0,15 mm. Surface roughness and internal clearances are also fixed to standard values.

The following stage variables are set free to be manipulated by the optimization algorithm: the specific diameter, the degree of reaction, the blade height to tip diameter ratio, the lap ratio, the axial solidity of nozzle and rotor blades and the number of nozzle and rotor blades. The numerical solution of the restrained optimization problem is achieved by the external penalty method, coupled with the Powell search algorithm. In general 6 to 9 restrained optimization iterations were needed to achieve solution convergence, corresponding respectively to about 15000 to 25000 stage performance calculations.

## 6. SIMULATION RESULTS

The expander stage performance is simulated under several cycle conditions indicated by the steam generator pressure, as shown in Tab. 1. The convergent profiled nozzle use is limited to a maximum evaporator temperature of 140ºC, condition which the stage has reached its limit aerodynamic load. The simulations with convergent-divergent profiled nozzles are extended to the supercritical conditions. The expander efficiency for both constructive alternatives analyzed is shown in figure 5. High efficiency is achieved for a single stage design at low evaporator pressure, as the viscous losses are diminished by the high local Reynolds numbers found in organic fluid service. The decreasing expander performance trend with steam generator pressure can be explained by the reduction of the specific speed, due to the increase in the specific enthalpy drop available and decrease of the circulated organic fluid mass flow, as shown in Tab. 1. This decreasing trend is seen to be steeper with the convergent profiled nozzle design. The reasons are clarified after examining the stage aerodynamic parameters. The stage degree of reaction, the axial acceleration factor and the rotor blade diffusion factor are shown in Fig. 6 and the absolute and relative flow Mach numbers are shown in Fig. 7, as function of steam generator pressure. In both graphics the convergent profiled nozzle results are plotted in blue as well the convergent-divergent profiled nozzles are plotted in black.

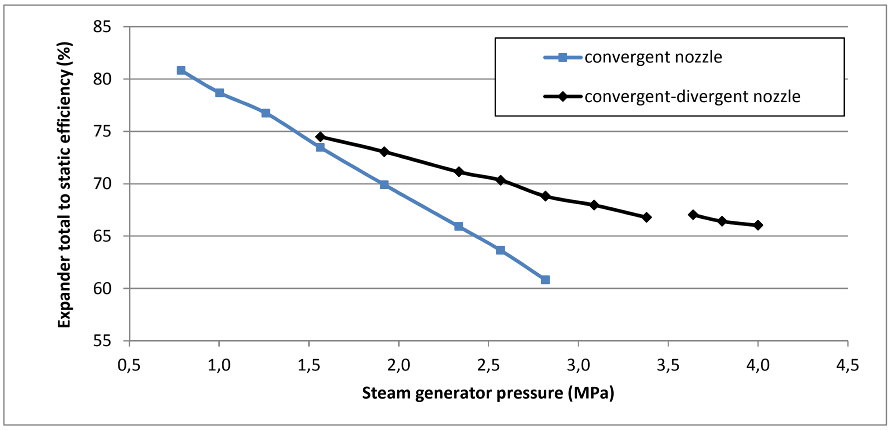


Figure 5. Expander total to static efficiency versus steam generator pressure for convergent and convergent-divergent profiled nozzle design.

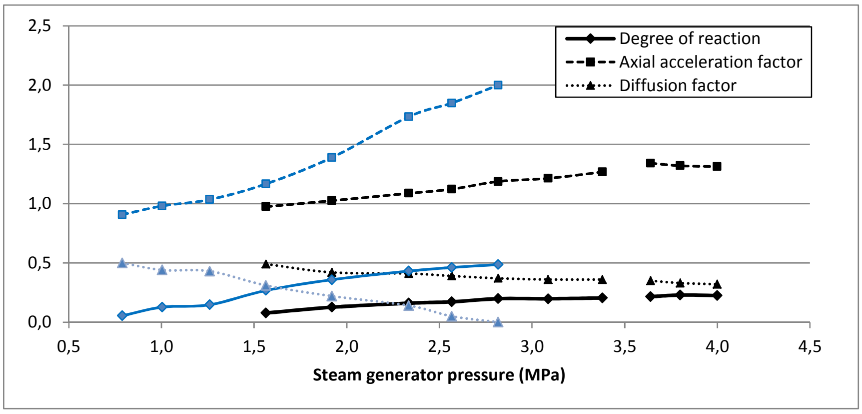


Figure 6. Degree of reaction, axial acceleration factor and rotor blade diffusion factor versus steam generator pressure for convergent profiled nozzle (in blue) and convergent-divergent profiled nozzle (in black).

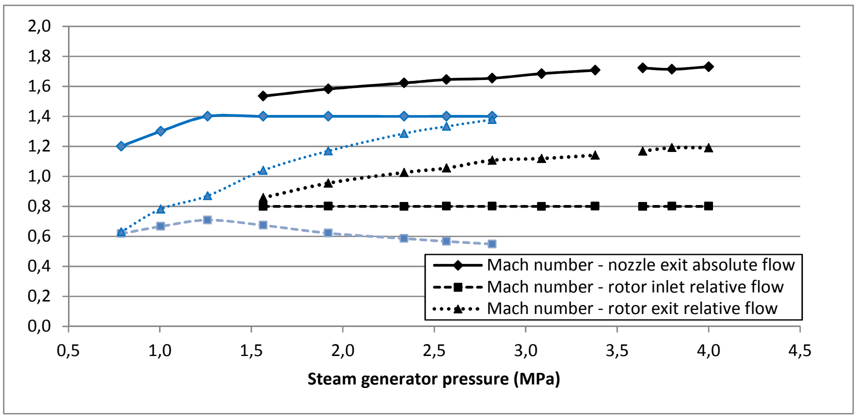


Figure 7. Mach numbers of nozzle exit absolute velocity, rotor inlet relative velocity and rotor exit relative velocity versus steam generator pressure for convergent profiled nozzle (in blue) and convergent-divergent profiled (in black).

For the stage equipped with convergent profiled nozzles the maximum aerodynamic load is reached in the nozzle blade row at an evaporator temperature of 100ºC and in the rotor blade row at an evaporator temperature of 140ºC. The degree of reaction and the axial acceleration factor are seen to be sharply increased with the steam generator pressure in order to keep the maximum Mach number restrictions. The result is a simultaneous increase of the exit kinetic energy loss and the corresponding decrease in performance.

A lower degree of reaction is shown to be enough to optimize the stage performance by the introduction of convergent-divergent profiled nozzles. In this case the performance decrease with steam generator pressure is less pronounced, once only a slight increase of the degree of reaction is needed and the exhaust losses are kept under control. In this case the Mach number of the inlet relative rotor velocity is seen to assume its maximum limit in the whole range of simulated cycle conditions.

The waste heat recovery cycle thermal efficiency is shown in Fig. 8 as function of steam generator pressure. Both the convergent profiled nozzle expander and the convergent-divergent profiled nozzle expander constructions are considered for the cycle performance calculation. The ideal cycle performance is also shown for comparison. In this case both the pump and the expander are considered isentropic machines.

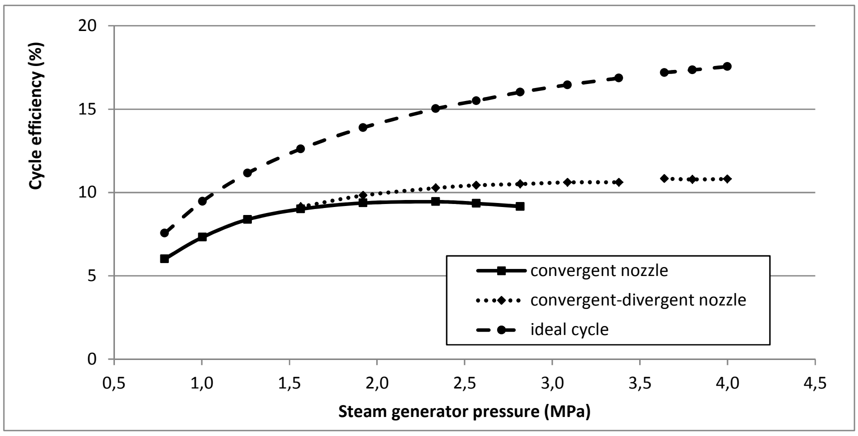


Figure 8. Organic Rankine cycle efficiency versus steam generator pressure.

The gross power produced by the expander-generator and the net power produced by the recovery cycle operating at subcritical conditions are shown in Fig. 9 for both constructive alternatives analyzed. Ideal cycle power results are also depicted for comparison. Once the amount of heat recovered is seen to decrease with evaporator temperature while the cycle efficiency is seen to increase, the maximum cycle net power produced is shown to take place at a determined optimum value. This optimum evaporator temperature is shown to assume different values according the constructive conception adopted. For the convergent profiled nozzle expander the optimum evaporator temperature is 120ºC and the net power is 148 kW, while for the convergent-divergent profiled nozzle expander the optimum evaporator temperature is 135ºC and the net power is 161 kW. The ideal cycle would present its best performance under evaporator temperature of 140ºC with a respective net power production of 242 kW.

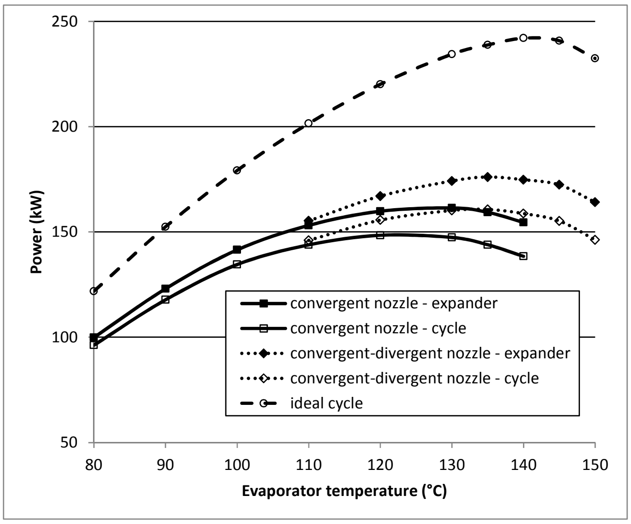


Figure 9. Expander generated power and cycle net output at subcritical cycle versus evaporator temperature.

## 7. CONCLUSIONS

The application of single stage axial expander to waste heat recovery ORC system is explored in the present work. Expander performance modeling is conducted under a preliminary design basis, incorporating real gas effects and a loss model based on the diffusion phenomena which takes place in the profile surfaces. A restrained optimization algorithm was successfully implemented to find the most efficient solution for each operating condition. The definition of compressibility constrains are taken under a challenging strategy, allowing the rotating blade row to be subjected to full aerodynamic loading. The performance simulation results shows that the single stage partial admission axial expander directly driving a two pole electrical generator is a possible solution for the ORC application under the fluid R245fa.

The high compressibility organic fluid media is found to have decisive importance over the single stage axial expander design. The convergent profiled nozzle stage is shown to be acceptable for subcritical cycle conditions, under an evaporator temperature below 140ºC. The performance is markedly impaired by evaporator temperature increase due to the kinetic energy exit loss. This result is consequence of the need to increase the stage degree of reaction in order to limit the nozzle exit Mach number. Therefore, the convergent-divergent profiled nozzle stage promises a better performance at high evaporator temperature or at supercritical cycle conditions.

The optimum value for the evaporator temperature at which the maximum net power output is produced by a subcritical cycle is shown to result from the decreasing trend of heat recovered and the increasing trend of cycle efficiency. The optimum value for the evaporator temperature is determined for the application proposed herein, taking into account the particular expander performance. The integrated optimization strategy is shown to be the most adequate approach to determine the maximum net output from the ORC system after the expander design conception is defined, as its efficiency will meaningfully affect the cycle performance.

## 8. REFERENCES

Baljé, O. E. and Binsley, R. L., 1968. “Axial Turbine Performance Evaluation. Part B: Optimization with and without Constraints”. Transactions of the ASME – Journal of Engineering for Power, Oct. 1968.

Baljé, O. E., 1968. “Axial cascade technology and Application to Flow Path Designs”. Transactions of the ASME-Journal of Engineering for Power, Oct. 1968.

Chao, H., Chao, L., Hong, G., Hui, X.,Yourong, L., Shuangying, W. and Jinliang, X., 2012. “The Optimal Evaporation Temperature and Working Fluids for Subcritical Organic Rankine Cycle”. Energy 38(2012).

Colonna, P., Nannan, N. R., Guardone, A. and Van der Stelt, T. P., 2009. Erratum to “On the Computation of the Fundamntal Derivative of Gas Dynamics Using Equation of State”. Fluid Phase equilibr. 286 (1) (2009) 43-54.

Dunavant, J. C. and Erwin, J. R., 1956. “ Investigation of a Related Series of Turbine-Blade Profiles in Cascade”. NACA TN-3802.

Lee, B. I. and Kesler, M. G., 1975. AiChe J., 21:510 (1975).

Luján, J. M., Serrano, J. R., Dolz, V. and Sánchez, J., 2012. “Model of the Expansion Process for R245fa in an Organic Rankine Cycle (ORC)”. Journal of Applied Thermal Engineering 40, 2012.

Macchi, E. and Perdichizzi, A., 1981. “Efficiency Prediction for Axial Flow Turbines Operating with Nonconventional Fluids”. Transactions of the ASME – Journal of Engineering for Power, Oct. 1981, vol. 103/719.

Martins, G. L., 2015. “Desempenho de Expansor axial de estagio Único e Admissão Parcial Aplicado a Ciclo Rankine Orgânico para Recuperação de Calor”. Tese de Doutorado, Departamento de Engenharia Mecânica, Pontifícia Universidade Católica do Rio de Janeiro.

Schuster, A., Karellas, A. and Aumann, R., 2009. “Efficiency Optimization Potential in Supercritical Organic Rankine Cycles”. Energy (2009), doi:10.1016/j.energy.2009.06.019.

Stewart, W. L., Whitney, W. J. and Miser, J. W., 1956. “Use of Effective Momentum Thickness in Describing Turbine Rotor Blade Losses”. NACA RM-E56B29.

Stewart, W. L., Whitney, W. J. and Wong, R. Y., 1960. “A Study of Boundary Layer Characteristics of Turbomachine Blade Rows and their relation to Overall Blade Losses”. Transactions of the ASME – Journal of Basic Engineering, Sept. 1960.

Wheeler, A. P. S. and Ong, J., 2013. “The Role of Dense gas dynamics on ORC Turbine Performance”. In *Proceedings of the ASME Turbo Expo 2013: Turbine technical Conference and Exposition* – GT2013-95858.

Zhdanov, I., Staudacher, S. and Falaleev, S., 2013. “An Advanced Usage of Meanline Loss Systems for Axial Turbine Design Optimization”. In *Proceedings of the ASME Turbo Expo 2013: Turbine technical Conference and Exposition* – GT2013-94323.

## 9. RESPONSIBILITY NOTICE